



**HAL**  
open science

# Low Power Thermodynamic Solar Energy Conversion: Coupling of a Parabolic Trough Concentrator and an Ericsson Engine

Muriel Alaphilippe, Sébastien Bonnet, P Stouffs

► **To cite this version:**

Muriel Alaphilippe, Sébastien Bonnet, P Stouffs. Low Power Thermodynamic Solar Energy Conversion: Coupling of a Parabolic Trough Concentrator and an Ericsson Engine. *International Journal of Thermodynamics*, 2007, 10 (1), pp.37-45. hal-04231706

**HAL Id: hal-04231706**

**<https://hal.science/hal-04231706>**

Submitted on 6 Oct 2023

**HAL** is a multi-disciplinary open access archive for the deposit and dissemination of scientific research documents, whether they are published or not. The documents may come from teaching and research institutions in France or abroad, or from public or private research centers.

L'archive ouverte pluridisciplinaire **HAL**, est destinée au dépôt et à la diffusion de documents scientifiques de niveau recherche, publiés ou non, émanant des établissements d'enseignement et de recherche français ou étrangers, des laboratoires publics ou privés.

## Low Power Thermodynamic Solar Energy Conversion: Coupling of a Parabolic Trough Concentrator and an Ericsson Engine

Muriel Alaphilippe, Sébastien Bonnet, Pascal Stouffs\*  
Laboratoire de Thermique, Energétique et Procédés  
Université de Pau et des Pays de l'Adour  
F-64000 PAU, France  
pascal.stouffs@univ-pau.fr

### Abstract

This paper considers thermodynamic conversion of solar energy into electric energy (up to maximum 50 kWe), presenting a very brief review of the possible systems: the 'Dish/Stirling' technology, which relies on high temperature Stirling engines and requires high solar energy; low temperature differential thermal engine using direct solar energy without any concentration but with very low power per unit volume or unit mass of the system; and the intermediate solar energy concentration ratio. A theoretical investigation on the coupling of a two-stage parabolic trough concentrator with a reciprocating Joule cycle air engine (*i.e.* an Ericsson hot air engine in open cycle) is presented. It is shown that there is an optimal operating point that maximises the mechanical power produced by the thermal engine. The interest of coupling a simple, low cost parabolic trough and a simple, low technology, mid- $\Delta T$  Ericsson engine is confirmed.

*Keywords: Solar energy, Ericsson engine, parabolic trough, Joule cycle engine*

### 1. Introduction

Due to environment problems, the conversion of solar energy into electricity is a very important energetic challenge. In this paper, thermodynamic conversion based on thermal engines working with external heat input is studied. Power levels considered here range from some hundreds watts up to about fifty kilowatts. This power range is chosen because it is of practical importance and because usual energy conversion systems based on turbomachinery are not suited to this low power level. A very brief survey about actual research and state of the art is presented. It seems that from the thermoeconomics point of view, the appropriate answer for low power solar energy conversion into electricity is presumably in the range of intermediate solar energy concentration ratio, and thus mid- $\Delta T$  engine (Bonnet et al., 2006). Therefore, a preliminary study on the coupling of a two-stage parabolic trough concentrator with a reciprocating Joule cycle air engine, *i.e.* an Ericsson hot air engine in open cycle is presented. These preliminary results confirm the interest of coupling a simple, low cost parabolic

trough and a simple, low technology, mid- $\Delta T$  Ericsson engine.

### 2. Review of the Possible Systems

A simplified classification of thermal machines has previously been proposed (Stouffs, 2002). This classification helps to identify the external heat input engines suitable for power solar energy conversion. A first criterion deals with the type of compression and expansion machine. There are mainly three kinds of machines: turbomachines, rotating volumetric machines, reciprocating volumetric machines. The first ones are only suitable for large mass flow rates and thus for large power levels. Indeed the efficiency of turbomachines drops dramatically for low power levels. Rotating volumetric machines are quite difficult to manufacture and the use as an expansion device of most of them, like screw machines, has not yet been fully assessed. So only reciprocating machines, *i.e.* thermal engines with piston/cylinder systems are considered.

Another criterion is the existence or not of valves isolating the compression and expansion machines during the pressure variation processes.

\*Author to whom correspondence should be

For external heat input thermal engines, this criterion allows us to distinguish the Stirling engine family (without valves) from the Ericsson engine family (with valves). Although less well known than Stirling engines, Ericsson engines could have important advantages, especially for low or medium temperature applications (Stouffs, 2002).

Thermal solar collectors can be classified according to their concentration ratio (Mills, 2004; Solarpaces, 2005):

- non-concentrating flat plate collector,
- line focus collector that concentrates solar radiation in one plane only, with medium-concentration ratio, such as a parabolic-trough collector,
- high concentration ratio point-focus collector such as a parabolic-dish collector

which respectively corresponds to low (< 100°C), medium (from 100°C to about 450°C), and high (> 450°C) temperature levels of the heated fluid.

Most current existing systems for low power thermodynamic solar energy conversion are based on the 'Dish/Stirling' technology (Bonnet et al., 2006; Stine and Diver, 1994) that relies on high temperature Stirling engines and requires a high solar energy concentration ratio. It is clear that these systems are quite heavy, leading to high costs. Especially the concentrator, the sun tracking system and the engine fixation at the concentrator focus are quite expensive. Also the high pressure high temperature engine requires expensive technology. *Figure 1* presents an example of such a system, able to produce 25 kW of electric power. Initially developed and tested by McDonnell Douglas and Southern California Edison, it was acquired by Stirling Energy Systems in 1996 (SES, 2006). This system, built in the years 1984-1985, is made up of a 10.57 metre equivalent diameter concentrator with an efficiency of  $\eta_{\text{conc}} = 0.88$ , a cavity receiver with an opening of 0.2 metre and an efficiency of 0.9 that leads to an overall solar energy collection efficiency of 0.79. The Stirling engine is a kinematics 4-95 MkII engine built by United Stirling AB (USAB). This engine has a 38-42% efficiency for a maximum hydrogen working fluid temperature of 720°C. The whole system leads to a global solar to electric energy conversion efficiency of 29-30%. This figure is more or less twice the efficiency of photovoltaic

cells, but the corresponding structure is obviously heavier.

Most solar dish/Stirling systems built up to now were based on pre-existing engines, usually developed for external combustion applications. This explains the high temperature level needed in the cavity receiver and therefore the high solar energy concentration level. These high temperature engines use high pressure (typically 20 MPa) helium or hydrogen as a working fluid. This is a quite high-tech, thus expensive, system.



*Figure 1. SES Dish/Stirling system*

However, it is possible to produce mechanical energy by means of a very low temperature differential thermal engine using direct solar energy without any concentration (Kongtragool and Wongwises, 2003; Bonnet et al., 2006). But obviously these systems produce very low power per unit volume or unit mass of the system.

We think that, from the thermoeconomics point of view, the appropriate answer for low power solar energy conversion into electricity is presumably in between, that is, in the range of intermediate solar energy concentration ratio and thus the mid- $\Delta T$  engine (Bonnet et al., 2006).

Our purpose is to examine the interest of this medium solution. Therefore, the coupling of a two-stage parabolic trough concentrator with a reciprocating Joule cycle air engine, *i.e.* an Ericsson hot air engine in open cycle) is studied. This analysis is developed in three successive steps: first a simplified analysis is achieved then a realistic model is developed, and finally a sensitivity analysis is realised.

### 3. Simplified Analysis

In a first step, a two-stage parabolic trough concentrator designed by Soleil-Vapeur (Boubour, 1996) (*Figure 2*) with an ideal receiver is considered. The solar energy is first concentrated by the cylindro-parabolic mirror in the lower part of the concentrator. The concentrated beams are then concentrated again by the so-called Compound Parabolic Concentrator (CPC) in the upper part of the system (Pramuang, 2005).

At the focal line of the concentrator, solar energy is transferred to air in the receiver heat exchanger. This heat exchanger receiver is placed on top of the CPC (*Figure 3*).

The optimal air mass flow rate through the receiver heat exchanger is determined.



Figure 2. Soleil-Vapeur concentrator

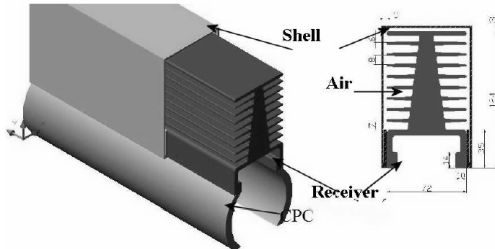


Figure 3. Air exchanger placed on the top of the CPC - detail of the receiver

Defining  $T_{rh}$  as the air temperature at the receiver inlet,  $T_h$  the air temperature at the receiver outlet, the heat power  $\dot{Q}_H$  recuperated by the air from the sun in the receiver (heater heat exchanger):

$$\begin{cases} \dot{Q}_H = \eta_{conc} L L_{N-S} E \\ \dot{Q}_H = \dot{m} c_p (T_h - T_{rh}) \end{cases} \quad (1)$$

From Equation (1), we derive:

$$T_h = \frac{\eta_{conc} L L_{N-S} E}{\dot{m} c_p} + T_{rh} \quad (2)$$

Considering  $1 - \frac{T_{rh}}{T_h}$  corresponding to the Carnot efficiency, the exergy stream is transferred by the concentrated solar beam into the receiver:

$$\begin{aligned} \dot{E}x_H &= \dot{Q}_H \left( 1 - \frac{T_{rh}}{T_h} \right) \\ &= \dot{Q}_H \left( 1 - \frac{T_{rh}}{\frac{\dot{Q}_H}{\dot{m} c_p} + T_{rh}} \right) \end{aligned} \quad (3)$$

In these relationships,  $T_{rh}$ ,  $c_p$ ,  $\dot{Q}_H$  do not depend on  $\dot{m}$ . Considering the positive constant  $a = \frac{c_p T_{rh}}{\dot{Q}_H}$ , the exergy stream with respect to the mass flow rate is derived:

$$\frac{d\dot{E}x_H}{d\dot{m}} = -\frac{\dot{Q}_H}{a} \frac{1}{\left(\frac{1}{a} + \dot{m}\right)^2} \quad (4)$$

The exergy stream derivative Equation.(4) is always negative. That means that the exergy flow rate in the air through the receiver is maximum when the air flow rate tends towards zero. From this result it follows that, for an ideal receiver, the negative effect of the  $T_h$  temperature decrease is more prejudicial than the effect of the mass flow rate increase from the exergetic stream point of view. So, according to this result, the largest mechanical power should be produced with an ideal receiver coupled with a thermal engine at very high (infinite) hot source temperature, but very low (zero) working fluid mass flow rate.

### 4. The Model

Then, a realistic model was developed in order to investigate the performance of the global system composed of the coupling of the two-stage parabolic trough concentrator with an Ericsson hot air engine. As shown in *Figure 4*, the Ericsson engine works in open cycle. The ambient air at  $P_0$  and  $T_k$  is first compressed in the compression space at  $P_{max}$ ,  $T_{cr}$ , then preheated in the recuperator to  $T_{rh}$ , then heated from the solar

beam through the concentrator to  $T_h$ . After that, air is expanded in the expansion space to  $P_0, T_{er}$ . Finally the expanded air gives thermal energy to the recuperator heat exchanger before being exhausted into the atmosphere at  $T_{rk}, P_0$ .

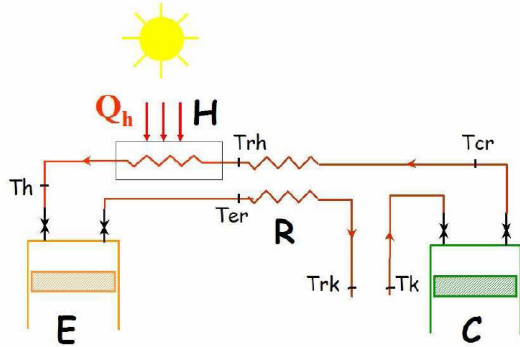


Figure 4. Solar concentrator coupled to Ericsson engine

Our work consists in designing a suitable engine for a given solar concentrator, and thus, in investigating the performance of the system as a function of the pressure ratio  $\beta$ , i.e. ( $P_{max} / P_0$ ) and the air mass flow rate in the engine. The main data considered for this analysis are given in TABLE I. A solar collector aperture area  $L \times L_{N-S} = 6.5 \text{ m}^2$  and a direct solar radiation  $E = 1000 \text{ W m}^{-2}$  is assumed. The optical efficiency of the concentrator is  $\eta_{conc} = 0.6$ . Convective and radiative heat losses are taken into account for the receiver. The approach is similar to the one developed by previous authors (Shawki and Eldighidy, 1993; Howell and Bannerot, 1976). However, the recuperative Joule cycle and the assumption of non-uniform wall and fluid temperature along the receiver heat exchanger axis considered in the present study lead to a much more complicated analysis.

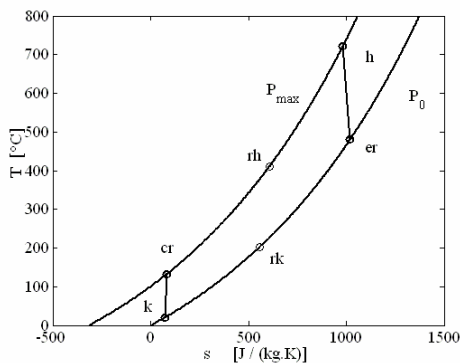


Figure 5. Temperature-entropy diagram of the proposed system

Figure 5 presents the successive thermodynamic processes of the air in a temperature-entropy diagram. Air is assumed to obey the perfect gas law with constant heat capacity. It can be seen that the compression and the expansion are assumed to be characterised by an isentropic efficiency  $\eta_{s,C} = \eta_{s,E} = 0.9$ . No pressure losses are taken into account for the air flow in the recuperator and heater heat exchangers. The recuperator heat exchanger effectiveness is  $\epsilon_r = 0.8$ . For convective thermal losses between receiver and ambient air, the convective heat transfer coefficient outside the receiver  $h_{free}$  is considered as a constant  $h_{free} = 10 \text{ W/m}^2\text{K}$ . Finally, mechanical losses are taken into account by means of mechanical efficiencies for the compression and the expansion device. It should be emphasised that the performance of the system deeply depends on the values chosen for the efficiencies  $\eta_{conc}, \eta_{s,C}, \eta_{s,E}, \eta_{mec,C}, \eta_{mec,E}$ . More theoretical but also mainly experimental work is needed to assess the efficiency values used in the model.

These assumptions lead to the following equations set. The net indicated power  $\dot{W}_i$  comes out as the difference between the expansion  $\dot{W}_{Ei}$  and compression  $\dot{W}_{Ci}$  indicated powers Equation (5), which are computed from Eqs. (6) and (7), where  $\dot{m}$  stands for the air mass flow rate in the Ericsson engine and where the specific heat of air is assumed to be constant:  $c_p = 1004 \text{ J kg}^{-1} \text{ K}^{-1}$ . The net shaft power  $\dot{W}_{shaft}$  comes out as the difference between the expansion  $\dot{W}_{Er}$  and compression net mechanical powers  $\dot{W}_{Cr}$  Equation (8), which take mechanical losses into account by means of the expansion and compression mechanical efficiencies Eqs. (9) and (10).

$$\dot{W}_i = \dot{W}_{Ei} - \dot{W}_{Ci} \quad (5)$$

$$\dot{W}_{Ci} = \dot{m} c_p (T_{cr} - T_k) \quad (6)$$

$$\dot{W}_{Ei} = \dot{m} c_p (T_h - T_{er}) \quad (7)$$

$$\dot{W}_{shaft} = \dot{W}_{Er} - \dot{W}_{Cr} \quad (8)$$

$$\dot{W}_{Cr} = \frac{\dot{W}_{Ci}}{\eta_{mec,C}} \quad (9)$$

$$\dot{W}_{Er} = \eta_{mec,E} \dot{W}_{Ei} \quad (10)$$

The temperatures at the end of the compression and expansion process  $T_{cr}$  and  $T_{er}$  are computed by means of the corresponding isentropic efficiencies and temperatures  $T_{cr,s}$  and  $T_{er,s}$  Eqs. (12) and (14). In Eqs. (11) and (13),  $k$  stands for  $(\gamma - 1)/\gamma$ , where the isentropic exponent  $\gamma = 1.4$ .

$$\frac{T_h}{T_{er,s}} = \beta^k \quad (11)$$

$$T_{er} = T_h - \eta_{si,E} (T_h - T_{er,s}) \quad (12)$$

$$\frac{T_{cr,s}}{T_k} = \beta^k \quad (13)$$

$$T_{cr} = T_k + \frac{T_{cr,s} - T_k}{\eta_{si,C}} \quad (14)$$

Temperatures in the thermodynamic cycle are also related by the recuperator balance Equation (15) and effectiveness  $\epsilon_r$  Equation (16).

$$T_{er} - T_{rk} = T_{rh} - T_{cr} \quad (15)$$

$$\epsilon_r = \frac{T_{rh} - T_{cr}}{T_{er} - T_{cr}} \quad (16)$$

The energy balance written on an elementary volume of the heater leads to the equations set (17) where  $T_{air}(x)$  and  $T_w(x)$  stand for local air and wall temperature in the heater.

$$\left\{ \begin{array}{l} \dot{m} c_p \frac{dT_{air}}{dx} = \eta_{conc} E L_{N-S} - h_{free} l_{pup} (T_w(x) - T_0) \\ \quad - \alpha \sigma F l_{pup} (T_w^4(x) - T_0^4) \\ \dot{m} c_p \frac{dT_{air}}{dx} = h_{conv} P_{MT} (T_w(x) - T_{air}(x)) \end{array} \right. \quad (17)$$

The left-hand member of both equations of system (17) corresponds to the thermal power transferred to the air flowing in the heater. The right-hand member of the first equation is made up of three terms: the first one computes the thermal power entering the cavity receiver; the second and the third ones take the convective and radiative losses into account. Finally, the right-hand member of the second equation expresses that the thermal power is transferred from the heater wall to the air by forced convection. The convective heat transfer coefficient is obtained from Equation (18) in which the Prandtl number is taken as  $Pr = 0.7$  and the air viscosity  $\mu = 2.08 \cdot 10^{-5} \text{ kg m}^{-1} \text{ s}^{-1}$ .

$$Re = \frac{\dot{m} D_M}{\mu S_p} ; \quad St = \frac{0.023}{(Re^{0.2} Pr^{0.6})} \quad (18)$$

$$h_{conv} = \frac{St c_p \dot{m}}{S_p}$$

Integration of system (17) on the heater length gives a relationship between  $T_{air}(x=0) = T_{rh}$  et  $T_{air}(x=L) = T_h$ . For the computation, the heater length has been divided into 10 parts of finite length. System (17) is solved numerically.

TABLE I. MAIN CHARACTERISTICS OF THE SYSTEM, AND DATA USED IN THE MODEL

Parameter	Symbol	Value
concentr. & receiver length	L	2.5 m
conc. north-south width	$L_{N-S}$	2.6 m
CPC output width	$l_{pup}$	0.04 m
optical conc. efficiency	$\eta_{conc}$	0.6
receiver absorbance	$\alpha$	1
view factor	F	0.15
receiver cross-section free area	$S_p$	$2.974 \cdot 10^{-3} \text{ m}^2$
wet perimeter	$P_M$	1.388 m
heat transfer perimeter	$P_{MT}$	1.057 m
compress. mech. efficiency	$\eta_{mec,C}$	0.9
expansion mech. efficiency	$\eta_{mec,E}$	0.9
isentropic comp. efficiency	$\eta_{si,C}$	0.9
isentropic exp. efficiency	$\eta_{si,E}$	0.9
recuperator effectiveness	$\epsilon_r$	0.8
direct solar radiation	E	$1 \text{ kW m}^{-2}$
ambient pressure	$P_0$	$10^5 \text{ Pa}$
ambient temperature	$T_0$	288 K

## 5. Results and Discussion

The pressure ratio considered here lies in the range  $1 \leq \beta \leq 4.8$  while the working air mass flow rate range is

$$0.0001 \text{ kg s}^{-1} \leq \dot{m} \leq 0.02 \text{ kg s}^{-1} .$$

Figure 6 presents the global efficiency of the system. It can be seen that there is a point that maximises the global efficiency, corresponding to  $\beta = 3.0$  and  $\dot{m} = 0.0085 \text{ kg s}^{-1}$ . The parameter values corresponding to that point are given in TABLE II. As observed in TABLE II, the intermediate solar energy concentration technology under consideration is fully adapted for micro-cogeneration. The thermal power coming from the sun across the concentrator aperture area is  $\dot{Q}_{\text{sun}} = (L L_{N-S} E) = 6500 \text{ W}$ . From that thermal power, due to the optical losses of the concentrator and the radiative and convective heat losses in the receiver, a thermal power of  $\dot{Q}_H = 2652 \text{ W}$  is transferred from the concentrated solar energy to the working air in the receiver (heater) heat exchanger H. The collector efficiency, defined as the ratio of the thermal power transferred to the air in the engine to the thermal power on the concentrator, is  $\eta_{\text{coll}} = \dot{Q}_H / \dot{Q}_{\text{sun}} = 0.408$ . It describes the quality of the system made up of the concentrator and the receiver. The relatively poor value of  $\eta_{\text{coll}}$  is mainly due to the low concentrator optical efficiency  $\eta_{\text{conc}}$  considered in this study.

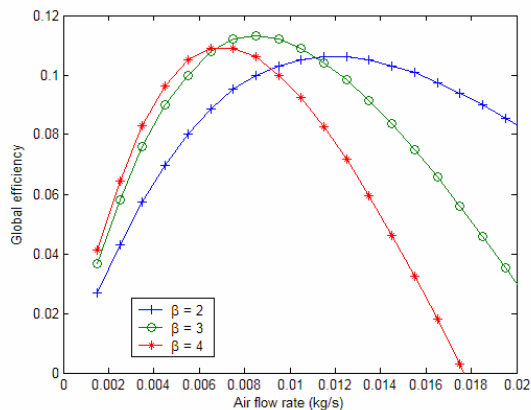


Figure 6. Global efficiency as a function of air mass flow rate and pressure ratio

The thermal power  $\dot{Q}_H$  transferred to the air produces an indicated power of  $\dot{W}_i = 1051 \text{ W}$ , corresponding to an indicated efficiency  $\eta_i = \dot{W}_i / \dot{Q}_H = 0.396$ . The mechanical losses have to be deducted from the indicated power so that the mechanical shaft power is  $\dot{W}_{\text{shaft}} = 733 \text{ W}$ . The global mechanical efficiency of the whole Ericsson engine is thus  $\eta_{\text{mec}} = \dot{W}_{\text{shaft}} / \dot{W}_i = 0.697$ . There is also a recoverable thermal power of  $\dot{Q}_K = 1601 \text{ W}$  in the air at the engine exhaust. The temperature of this air is  $T_{\text{rk}} = 203 \text{ }^\circ\text{C}$ . This level is high enough for the cogeneration process. The fluid at the engine exhaust is pure, clean air.

Finally, the global efficiency, defined as the ratio of the shaft power to the thermal power from the sun, is  $\eta_{\text{Global}} = \dot{W}_{\text{shaft}} / \dot{Q}_{\text{sun}} = 0.113$ . This value can be considered as relatively low compared to those obtained from the Dish/Stirling technology, but the whole system will be cheaper, and that global efficiency can easily be increased, for instance, by improving the concentrator optical efficiency.

TABLE II. PERFORMANCE AT THE OPERATING POINT

Symbol	Value	Symbol	Value
$\beta$	3	$\dot{Q}_{\text{sun}}$	6500 W
$\dot{m}$	$0.0085 \text{ kg s}^{-1}$	$\dot{Q}_H$	2652 W
$T_k$	288 K	$\dot{W}_i$	1051 W
$T_{\text{cr}}$	406 K	$\dot{W}_{\text{shaft}}$	733 W
$T_{\text{rh}}$	684 K	$\dot{Q}_K$	1601 W
$T_h$	995 K	$\eta_{\text{coll}}$	0.408
$T_{\text{er}}$	754 K	$\eta_i$	0.396
$T_{\text{rk}}$	476 K	$\eta_{\text{mec}}$	0.697
		$\eta_{\text{Global}}$	0.113

Figure 7 shows the mechanical shaft power as a function of the air mass flow rate for different values of the pressure ratio. As in Figure 6, the optimal point that maximises the whole system performance appears clearly.

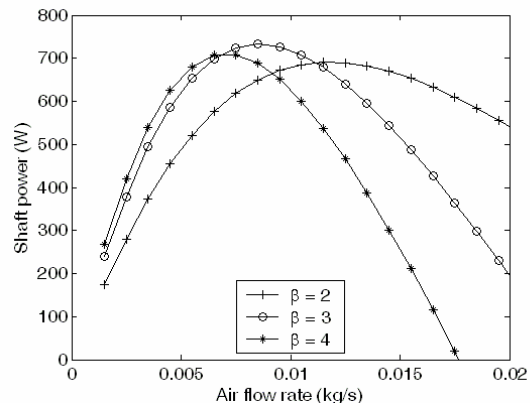


Figure 7. Shaft power as a function of air mass flow rate for several pressure ratios

Figure 8 shows that, as the air flow rate decreases, the air temperature at the heater outlet tends towards a stagnation temperature independent on the pressure ratio. For a given air flow rate, the inlet and outlet air temperature in the heater increases as the pressure ratio decreases. Figure 9 shows the receiver efficiency, defined as the ratio of the heat power transferred to the working fluid in the receiver heat exchanger to the concentrated solar power

entering the receiver. As expected, the efficiency drops dramatically as the air flow rate decreases. For pressure ratios larger than  $\beta = 2$ , the influence of the pressure ratio is low.

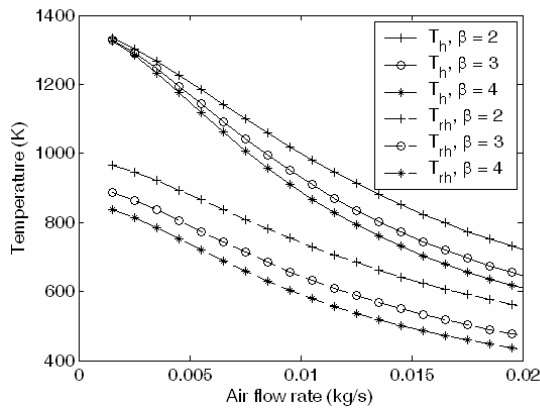


Figure 8. Inlet and outlet air temperature in the heater as a function of air flow rate

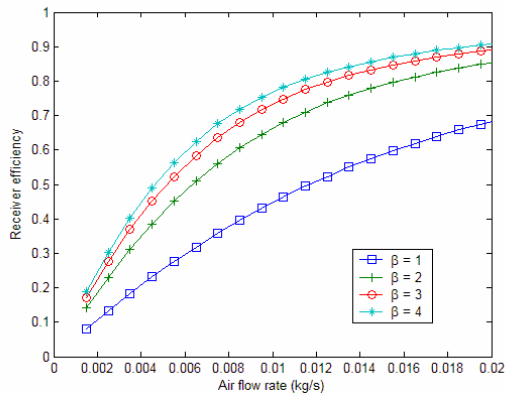


Figure 9. Receiver efficiency as a function of air mass flow rate and pressure ratio

## 6. Sensitivity Analysis

A parametric study shows the influence of such data as the solar radiation, the concentrator optical efficiency, the ambient temperature, the mechanical component efficiencies and the recuperator effectiveness.

### 6.1. Solar radiation and concentrator optical efficiency ( $\eta_{\text{conc}} \times E$ )

The concentrator optical efficiency  $\eta_{\text{conc}}$  and the direct solar radiation  $E$  always appear as a product in the model (Equation 17). The influence of these parameters can thus be studied simultaneously. Figure 10 shows that their impact on the shaft power is very important, as the thermal power available in the heater for the engine directly depends on the product  $\eta_{\text{conc}} \times E$ .

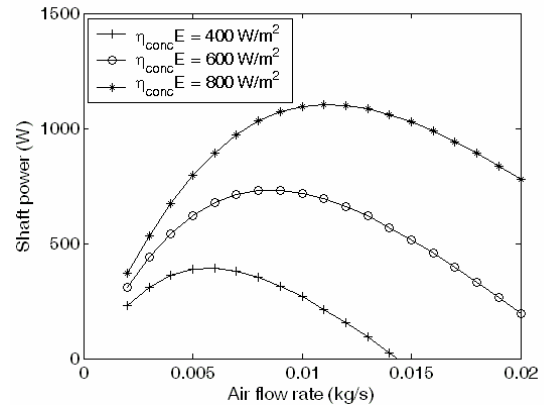


Figure 10. Shaft power for several values of the product of the solar radiation by the optical efficiency

### 6.2. Ambient temperature $T_0$

For the temperatures considered ( $T_0 = 15^\circ\text{C}$  and  $T_0 = 0^\circ\text{C}$ ), Figure 11 shows that the ambient temperature does not affect the shaft power very much. Two phenomena are in competition: the cycle thermodynamical efficiency increases as the ambient temperature decreases, but the heater radiative and convective thermal losses also increases. This latter effect is less pronounced than the first one for the temperatures considered.

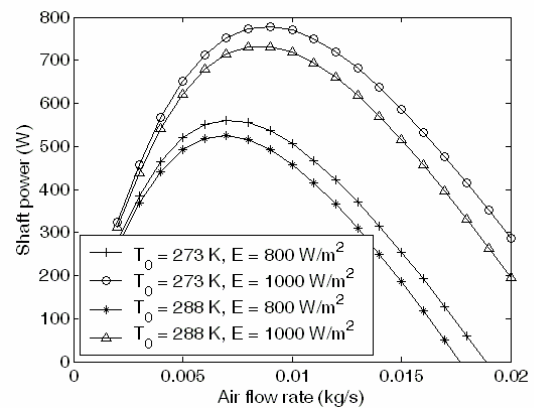


Figure 11. Shaft power for several values of the ambient temperature and the solar radiation

### 6.3. Component mechanical efficiencies

The model used (Eqs. 5, 6) leads to bad performance as soon as the indicated expansion power  $\dot{W}_{Ei}$  tends towards the indicated compression power  $\dot{W}_{Ci}$ , that is as the pressure ratio  $\beta$  gets lower. The pressure ratio considered here is quite low ( $\beta = 3$ ). It is thus very important to have a short and efficient kinematic drive linking the expansion and the compression



pistons, in order to achieve good mechanical efficiencies. This is confirmed by *Figure 12*. Also, the model and the value for the mechanical efficiency should be assessed.

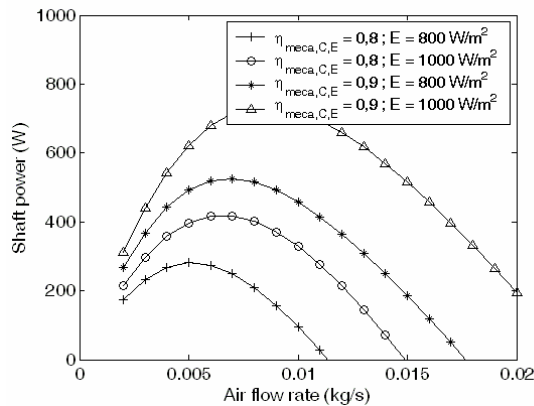


Figure 12. Shaft power for several values of the mechanical efficiencies

#### 6.4. Recuperator effectiveness $\epsilon_r$

The recuperator heat exchanger area directly depends on the recuperator effectiveness  $\epsilon_r$ . *Figure 13* has been drawn for a lower recuperator effectiveness, *i.e.*  $\epsilon_r = 0.5$  instead of  $\epsilon_r = 0.8$ . By comparison with *Figure 7*, it can be seen that the shaft power suffers a decrease as the recuperator effectiveness gets lower. It is very important to design a recuperator with a large effectiveness. It can also be seen that the optimal engine pressure ratio  $\beta$  gets higher as the recuperator effectiveness gets lower, which is an expected result. On the other hand, the optimal air mass flow rate in the engine decreases as the effectiveness decreases, leading to higher temperature difference ( $T_h - T_m$ ) between the heater inlet and outlet.

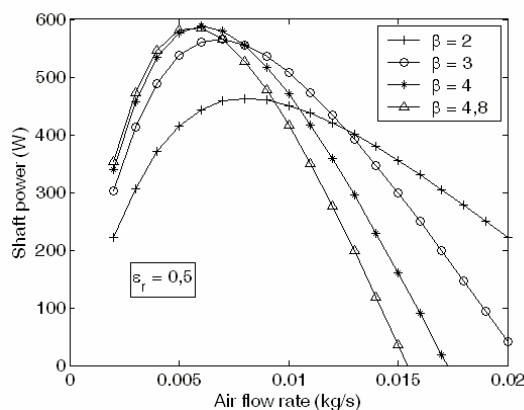


Figure 13. Shaft power for a recuperator with a lower effectiveness

## 7. Conclusion

The coupling of a parabolic trough solar concentrator with a hot air Ericsson engine in open cycle has been modeled. According to the results from the model, with a  $6.5 \text{ m}^2$  solar collector aperture area and a direct solar radiation  $E = 1000 \text{ W m}^{-2}$ , the proposed system produces a maximum shaft power of about  $733 \text{ W}$  and a recoverable thermal power of  $\dot{Q}_K = 1601 \text{ W}$  at  $T_{rk} = 203^\circ\text{C}$ . The engine thermodynamic design leads to realistic and convenient dimensional characteristics. These preliminary results confirm the interest of coupling a simple, low cost parabolic trough and a simple, low technology, mid- $\Delta T$  Ericsson engine. The further step will be to build a prototype to validate the very promising results found here. The system from the exergo-economic point of view (Bejan et al., 1996), in order to assess its interest according to local conditions of sunshine and energy accessibility and cost, has to be investigated.

## Nomenclature

$c_p$	specific heat at const. pressure [ $\text{J kg}^{-1} \text{K}^{-1}$ ]
$D_M$	hydraulic diameter in the receiver [m]
$E$	beam normal solar radiation [ $\text{W m}^{-2}$ ]
$\dot{E}_X$	exergy stream [W]
$F$	view factor [-]
$h_{\text{conv}}$	convective heat transfer coefficient in the receiver [ $\text{W m}^{-2} \text{K}^{-1}$ ]
$h_{\text{free}}$	convective heat transfer coefficient outside the receiver [ $\text{W m}^{-2} \text{K}^{-1}$ ]
$k$	$(\gamma - 1) / \gamma$
$L$	concentrator length [m]
$L_{N-S}$	concentrator North-South width [m]
$l_{\text{pup}}$	CPC output width [m]
$\dot{m}$	working fluid air flow rate [ $\text{kg s}^{-1}$ ]
$P$	pressure [Pa]
$P_M$	wet perimeter in the receiver [m]
$P_{MT}$	heat transfer perimeter in the receiver [m]
$Pr$	Prandtl number [-]
$\dot{Q}$	heat power [W]
$Re$	Reynolds number [-]
$S_p$	cross-sectional free area in receiver [ $\text{m}^2$ ]
$St$	Stanton number [-]
$T$	temperature [K]
$\dot{W}$	mechanical power [W]
$x$	coordinate along the heat exchanger [m]

## Greek letters

$\alpha$	receiver absorbance [-]
$\beta$	compression ratio [-]
$\gamma$	specific heat ratio $c_p/c_v$ [-]
$\epsilon_r$	recuperator thermal effectiveness [-]

$\eta$	efficiency [-]
$\mu$	dynamic viscosity [ $\text{kg m}^{-1} \text{s}^{-1}$ ]
$\sigma$	Stefan-Boltzman constant [ $\text{W m}^{-2} \text{K}^{-4}$ ]

### Subscripts

air	air (as the working fluid)
C	compression cylinder
coll	collector (concentrator + receiver)
conc	concentrator
E	expansion cylinder
Glob	global
H	heater (receiver)
i	indicated
K	rejected at the cold sink
mec	mechanical
r	real (net value)
s	isentropic
shaft	shaft
sun	received from the sun
w	wall
0	ambient state

### References

- Bejan A., Tsatsaronis G., Moran M., 1996, *Thermal design and optimization*, John Wiley and Sons ed., NY, USA.
- Bonnet S., Alaphilippe M., Stouffs P., 2006, "Thermodynamic solar energy conversion: Reflections on the optimal solar concentration ratio", *International Journal of Energy, Environment and Economics*, Vol. 12, No 3, pp. 141-152.
- Boubour J., 1996, "Demande de brevet d'invention: Capteur solaire linéaire à suivi discontinu", No 2754592, INPI, Paris.

Howell J. R., Bannerot R. B., 1976, "Optimum solar collector operation for maximizing cycle work output", *Solar Energy*, Vol. 19, pp. 149-153.

Kongtragool Bancha, Wongwises Somchai, 2003, "A review of solar-powered Stirling engines and low temperature differential Stirling engine", *Renewable and sustainable Energy Reviews*, Vol. 7, pp. 131-134.

Mills D., 2004, "Advances in solar thermal electricity technology", *Solar Energy*, Vol. 76, pp. 19-31.

Pramuang S., Exell R. H. B, 2005, "Transient test of a solar air heater with a compound parabolic concentrator", *Renewable energy*, Vol. 30, No 5, pp. 715-728.

SES, 2006, <http://www.stirlingenergy.com>

Shawki M. Eldighidy, 1993, "Optimum outlet temperature of solar collector for maximum work output for an OTTO air standard cycle with ideal regenerator", *Solar Energy*, Vol. 51, No 3, pp. 175-182.

Solarpaces, 2005, Concentrating Solar Power and Chemical Energy systems, <http://www.solarpaces.org>.

Stine W.B., Diver R.B, 1994, "A compendium of solar Dish/Stirling Technology", Sandia National Laboratories, Report SAND-7026 UC-236, USA.

Stouffs P., 2002, "Does the Ericsson engine deserve more consideration than the Stirling engine?" *Proceedings of the European Stirling Forum 2002*, Osnabrück, Germany.